forearc and subvertical realignment in the wedge. However, their modeling did not include both slab dip and plate rollback, thus preventing direct comparison to the Tonga backarc. There is, however, geochemical evidence to suggest that along-arc mantle flow is occurring in this area. A change in Fiji magmatism from arc-like to ocean island basalt was attributed to influx of the Samoan Plume around 3 million years ago (*35*). A similar explanation for high Nb relative to other high-field-strength elements in lavas at the islands Tafehi and Niuatoputapu at the northern end of the Tonga-Kermadec subduction zone was also proposed (*36*). In addition, helium isotope data suggest flow of the Samoan Plume magma toward the Peggy Ridge at the northern end of the Lau basin (*37*). Later mapping by Turner and Hawkesworth (*38*) mapped the presence of these high ^{3}He:^{4}He further south into the Lau backarc. Such isotope signatures, which are characteristic of the Samoan Plume, may be evidence of the flow of shallow mantle (*38*) from the Samoan Plume into the Lau basin, parallel to the trench, through a tear in the subducting Pacific plate (Fig. 5). These results match both the geographical locations of our stations and the azimuth of mantle flow we would infer from our anisotropy observations. We infer, therefore, that the observations of along-arc fast anisotropy axes reflect this geochemical mapping of along-arc mantle flow and are probably resulting from slab rollback and the along-strike component of the absolute plate motions.

References and Notes

1. Seismic anisotropy is the phenomenon in which the velocity of a seismic wave through a medium depends on the wave's polarization or propagation direction.
2. N. I. Christensen, *Geophys. J. R. Astron. Soc.* **76**, 89 (1984).
3. S. Zhang, S. Karato, *Nature* **375**, 774 (1995).
4. A. Tommasi, *Earth Planet. Sci. Lett.* **160**, 1 (1998).
5. M. Bystricky, K. Kunze, L. Burlini, J. P. Burg, *Science* **290**, 1564 (2000).
6. N. M. Ribe, *J. Geophys. Res.* **94**, 4213 (1989).
7. M. K. Savage, *Rev. Geophys.* **37**, 65 (1999).
8. D. McKenzie, *Geophys. J. R. Astron. Soc.* **58**, 689 (1979).
9. J. R. Bowman, M. Ando, *Geophys. J. R. Astron. Soc.* **88**, 25 (1987).
10. K. M. Fischer, D. A. Wiens, *Earth Planet. Sci. Lett.* **142**, 253 (1996).
11. M. J. Fouch, K. M. Fischer, *J. Geophys. Res.* **101**, 15987 (1996).
12. K. M. Fischer, M. J. Fouch, D. A. Wiens, M. S. Boettcher, *Pure Appl. Geophys.* **151**, 463 (1998).
13. C. E. Hall, K. M. Fischer, E. M. Parmentier, *J. Geophys. Res.* **105**, 28009 (2000).
14. E. a. J. N. Sandvol, *J. Geophys. Res.* **102**, 9911 (1997).
15. W. Alvarez, *J. Geophys. Res.* **87**, 6697 (1982).
16. R. M. Russo, P. G. Silver, *Nature* **263**, 1105 (1994).
17. K. Gledhill, D. Gubbins, *Phys. Earth Planet. Int.* **95**, 227 (1996).
18. V. Peyton *et al.*, *Geophys. Res. Lett.* **28**, 379 (2001).
19. J. Buttles, P. Olson, *Earth Planet. Sci. Lett.* **164**, 245 (1998).
20. K. M. Fischer, M. Parmentier, A. R. Stine, E. R. Wolf, in preparation.
21. D. K. Blackman *et al.*, *Geophys. J. Int.* **127**, 415 (1996).
22. H. H. Hess, *Nature* **203**, 629 (1964).
23. C. J. Wolfe, S. C. Solomon, D. R. Toomey, D. W. Forsyth, *Eos* **77**, F653 (1996).
24. C. J. Wolfe, P. G. Silver, *J. Geophys. Res.* **103**, 749 (1998).
25. I. T. Bjarnason, C. J. Wolfe, S. C. Solomon, G. Gudmundson, *Geophys. Res. Lett.* **23**, 459 (1996).
26. D. W. Forsyth, S. C. Webb, L. M. Dorman, Y. Shen, *Science* **280**, 1235 (1998).
27. Seismic instruments are composed of three orthogonal components: one vertical and two horizontal. Land stations are normally oriented so that one horizontal component is east-west and the other is north-south. OBS instruments are not emplaced by hand, and so the orientations of the horizontal components are not known a priori.
28. E. A. Flinn, *Proc. IEEE* **53**, 1874 (1965).
29. S-wave splitting is the observation of two S-wave arrivals with orthogonal polarization due to anisotropy. The splitting time is the time between the arrivals. The fast azimuth corresponds to the polarization azimuth of the first arriving S wave.
30. P. N. Chopra, M. S. Paterson, *J. Geophys. Res.* **89**, 7861 (1984).
31. H. Jung, K.-H. Lee, S.-i. Karato, *Eos* **81**, S53 (2000).
32. J.-M. Kendall, *Geophys. Res. Lett.* **21**, 301 (1994).
33. M. E. Zimmerman, S. Zhang, D. L. Kohlstedt, S. Karato, *Geophys. Res. Lett.* **26**, 1505 (1999).
34. M. J. Fouch, K. M. Fischer, *Geophys. Res. Lett.* **25**, 1221 (1998).
35. J. Gill, P. Whelan, *J. Geophys. Res.* **94**, 4579 (1989).
36. J. I. Wendt, M. Regelous, K. D. Collerson, A. Ewart, *Geology* **25**, 611 (1997).
37. R. J. Poreda, H. Craig, *Earth Planet. Sci. Lett.* **113**, 487 (1992).
38. S. Turner, C. Hawkesworth, *Geology* **26**, 1019 (1998).
39. M. Bevis *et al.*, *Nature* **374**, 249 (1995).
40. A. E. Gripp, R. G. Gordon, *Geophys. Res. Lett.* **17**, 1107 (1990).

3 January 2001; accepted 19 March 2001

Detection of Widespread Fluids in the Tibetan Crust by Magnetotelluric Studies

Wenbo Wei,[1] Martyn Unsworth,[2]* Alan Jones,[3] John Booker,[4] Handong Tan,[1] Doug Nelson,[5] Leshou Chen,[1] Shenghui Li,[4] Kurt Solon,[5] Paul Bedrosian,[4] Sheng Jin,[1] Ming Deng,[1] Juanjo Ledo,[3] David Kay,[4] Brian Roberts[3]

Magnetotelluric exploration has shown that the middle and lower crust is anomalously conductive across most of the north-to-south width of the Tibetan plateau. The integrated conductivity (conductance) of the Tibetan crust ranges from 3000 to greater than 20,000 siemens. In contrast, stable continental regions typically exhibit conductances from 20 to 1000 siemens, averaging 100 siemens. Such pervasively high conductance suggests that partial melt and/or aqueous fluids are widespread within the Tibetan crust. In southern Tibet, the high-conductivity layer is at a depth of 15 to 20 kilometers and is probably due to partial melt and aqueous fluids in the crust. In northern Tibet, the conductive layer is at 30 to 40 kilometers and is due to partial melting. Zones of fluid may represent weaker areas that could accommodate deformation and lower crustal flow.

The Tibetan plateau is the largest area of thickened and elevated continental crust on Earth and a direct consequence of the ongoing India-Asia collision (*1*). Knowledge of the structure and evolution of the plateau has advanced through modern geophysical studies that began in the 1980s with a Sino-French collaboration. Magnetotelluric (MT) data collected during this project detected unusually high electrical conductivity in the crust of southern Tibet (*2*). In combination with elevated heat flow (*3*), this was attributed to the presence of partial melt at shallow depths in the crust. In 1995, Project INDEPTH (*4*) acquired MT data in southern Tibet with the use of more advanced instrumentation and data-processing techniques (Fig. 1) (*5*). These data confirmed the existence of a high-conductivity zone at a depth of 15 to 20 km in southern Tibet that was coincident with seismic bright spots and a seismic low-velocity zone (*6*–*8*). These observations gave additional support to the idea that the high-conductivity layer represents partial melt in the Tibetan crust (*9*).

However, both of these MT surveys (*2*, *5*) were located within the Yadong-Gulu rift, one of the north-south–trending rifts that accommodate the ongoing east-west extension in southern Tibet (*10*). To determine if the conductive crust was limited to the rifts, we collected additional MT data in 1998 and 1999 (500 and 600 lines, Fig. 1). A charac-

[1]Department of Applied Geophysics, China University of Geosciences, Beijing, People's Republic of China. [2]Institute of Geophysical Research, University of Alberta, Edmonton, Alberta T6G 2JI, Canada. [3]Geological Survey of Canada, Ottawa, Canada. [4]Geophysics Program, University of Washington, Seattle, WA 98195, USA. [5]Geological Sciences, Syracuse University, Syracuse, NY 13244, USA.

*To whom correspondence should be addressed.

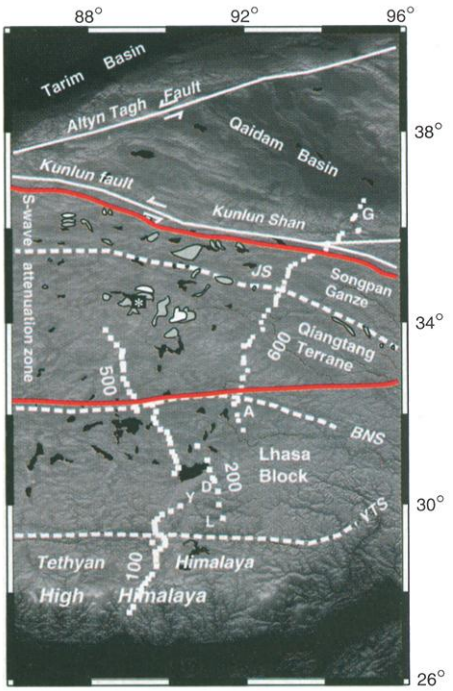

Fig. 1. Tectonic setting of the INDEPTH MT profiles. The numbers indicate the name of each profile. Y, Yangbaijin; D, Damshung; L, Lhasa; A, Amdo; G, Golmud; YTS, Yarlung Tsangpo suture; BNS, Bangong-Nuijang suture; JS, Jinsha suture. White denotes volcanic rocks younger than 5 million years and light gray denotes volcanic rocks older than 5 million years or undated (*32*). The asterisk denotes the xenolith location described by (*32*). The red lines are the limits of the zone of shear wave attenuation.

teristic feature of the MT data is that the apparent resistivities decrease with decreasing frequency, implying that conductivity increases with depth (*11*). This response was observed at most MT sites in Tibet and is markedly different from that observed in stable continental regions worldwide. The MT data from each profile were then converted into two-dimensional (2D) conductivity models (*12*). The most prominent feature observed in these models is that the crust is highly conductive across the entire plateau. The conductance of the Tibetan crust is one to two orders of magnitude higher than in stable continental regions (*13*, *14*).

In Fig. 2, the high Himalayan crystalline rocks appear as a low-conductivity (resistive) feature above the main Himalayan thrust (MHT). Below the MHT is a more conductive zone that extends to ~28.5°N, which is presumably the Indian continental crust underthrusting southern Tibet (*15*). The Indian crust beneath the MHT has a conductivity of 0.01 to 0.02 S/m, consistent with MT studies in Nepal (*16*). North of 28.5°N, the electrical signature of the Indian plate at depth disappears, and the crustal conductance increases to ~20,000 S in the vicinity of the Yarlung-Zangbo suture. Farther north, the top of the midcrustal conductor shallows to ~15 km beneath the Lhasa block, where it is coincident with seismic bright spots (*6*). Zones of high conductivity locally approach the surface at 29.7°N in an area of geothermal activity (*17*). In Fig. 3, the top of the midcrustal conductor then deepens to ~40 km beneath the southern Qiangtang terrane (~33.5°N on the 500 line). On the 600 line, the conductor shallows again to ~25 km beneath the central Qiangtang terrane and conductance rises (~33.5°N), where Plio-Pleistocene volcanic rocks are abundant along strike to the west (*18*). Modeling studies indicate that the conductor in this region extends to the base of the crust and perhaps into the upper mantle. Beneath the northern Qiangtang and Songpan-Ganze terranes, the conductor is confined above resistive upper mantle (60 to 100 km depth). This resistive structure could be Asian lithosphere underthrusting the northern edge of the Tibetan plateau (*19*, *20*).

Interconnected metallic ores, carbon films, partial melt, and aqueous fluids can all produce high crustal conductivities. Although metallic ore bodies can produce very high conductivities, they do not have spatial dimensions comparable to those observed in Tibet. Interconnected graphite films have been suggested as a cause for the elevated conductivity of the lower crust observed in cratons, but it is unlikely that graphite would be an effective conductor in the high-temperature regime beneath Tibet (*21*). Thus, the preferred explanation for the high conductance beneath Tibet is interconnected fluid, either partial melt or aqueous fluids present along the grain boundaries of the rock. The bulk conductivity of a fluid-bearing rock depends on the conductivity of the fluid, its geometry, and the amount of fluid. Laboratory measurements have shown that basaltic,

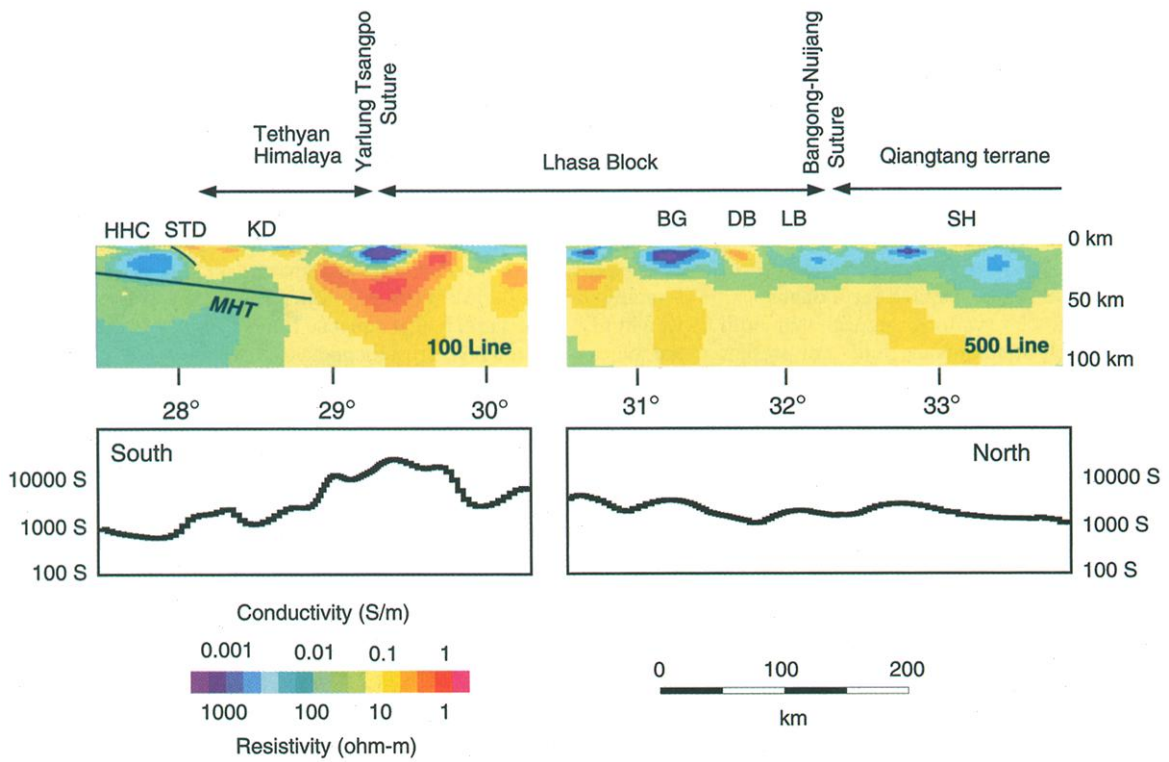

Fig. 2. Electrical conductivity models for the 100 line and the 500 line. HHC, high Himalayan crystalline units; KD, Kangmar dome; BG, Bangoin granite; DB, Duba basin; LB, Lumpola Basin; SH, Shuang Hu; STD, South Tibetan Detachment. The bottom panels show the conductance to 100 km.

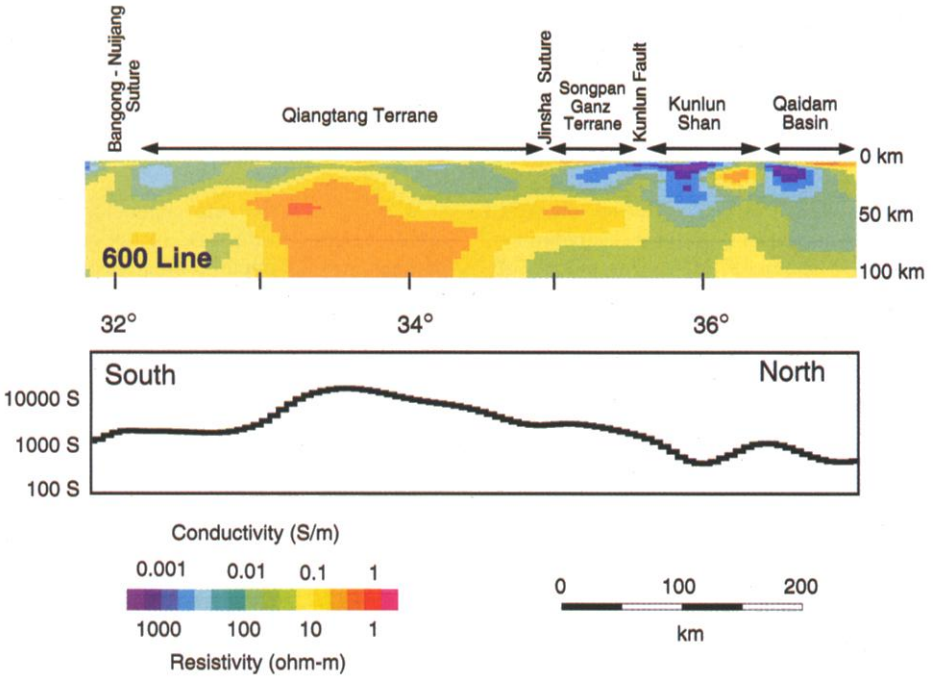

Fig. 3. Electrical conductivity model for northern Tibet (600 line).

andesitic, and granitic melts have electrical conductivities ranging from about 4 to 10 S/m (*22*, *23*). The melt phase generally becomes interconnected at low melt fractions (*24*) and lowers the overall conductivity of the rock (*25*). For example, 10% melt by volume with a conductivity of 10 S/m (at the upper limit) could yield a bulk conductivity of 0.6 S/m. A layer of this rock with 10% melt would need to be 16 km thick to produce a conductance of 10,000 S. Aqueous fluids can be more conductive than melt, and samples from geothermal fields and fluid inclusions show conductivities in excess of 100 S/m (*26*). A layer of aqueous fluids could produce the conductance observed in Tibet with a lower fluid fraction and/or layer thickness than considered above for partial melt. For example, a layer only 1.6 km thick containing 10% of 100 S/m brine would be needed to yield the observed 10,000-S conductance.

Several observations suggest that both partial melt and aqueous fluids are present in the crust of southern Tibet. The upper part of the high-conductivity zones (<15 km) in southern Tibet on the 100 line is associated with geothermal activity (*17*) and is probably due to aqueous fluids. The deeper parts of the high-conductivity zones may be due to partial melt because satellite magnetic data (*27*), high heat flow (*3*), and young granites (*28*) all indicate high crustal temperatures. A combination of aqueous fluids overlying a zone of partial melting is also indicated by the waveform of seismic waveforms from the top of the fluid layer (*7*). Radiogenic heating has generated the elevated temperatures needed to initiate partial melting during the process of crustal thickening (*29*).

The conductive zone in northern Tibet extends to greater depth than in southern Tibet. Laboratory studies suggest that at these depths, aqueous fluids will not connect to form conductive pathways (*30*) and, thus, partial melting is the most likely cause of the high conductivity. A conductive upper mantle is consistent with the Plio-Pleistocene volcanic rocks in this area being mantle derived, perhaps as a result of delamination (*1*). The conductive upper mantle is coincident with a region of low seismic velocities and high attenuation in northern Tibet (*31*); both seismic and electrical properties are as expected if partial melt were present. Xenoliths in 3-million-year-old volcanic rocks from northern Tibet show evidence of heating to 1350°C in the presence of basaltic melt and are essentially dry, with less than 1% water by weight (*32*). It is unlikely that aqueous fluids are the cause of the high crustal conductivity in northern Tibet. In contrast, basaltic melt is an obvious explanation for the high conductivity. The geometry of the high-conductivity feature at 34°N is suggestive of localized upwelling within the asthenosphere (*1*) and is bounded on the north and the south by relatively resistive zones that may indicate where Asian and Indian lithosphere descends.

References and Notes

1. P. Molnar, P. England, J. Martinod, *Rev. Geophys.* **31**, 357 (1993).
2. P. Van Ngoc *et al.*, *Nature* **319**, 310 (1986).
3. J. Francheteau *et al.*, *Nature* **307**, 32 (1984).
4. Project INDEPTH is International Deep Profiling of Tibet and the Himalaya.
5. L. Chen *et al.*, *Science* **274**, 1694 (1996).
6. L. D. Brown *et al.*, *Science* **274**, 1688 (1996).
7. Y. Makovsky, S. L. Klemperer, *J. Geophys. Res.* **104**, 10795 (1999).
8. R. Kind *et al.*, *Science* **274**, 1692 (1996).
9. K. D. Nelson *et al.*, *Science* **274**, 1684 (1996).
10. R. Armijo, P. Tapponier, P. Mercier, J. H. Tonglin, *J. Geophys. Res.* **91**, 13803 (1986).
11. Broadband MT data to image upper crustal structure (1000 to 0.01 Hz) and low-frequency MT data to image the lower crust and mantle (0.1 to 0.00003 Hz) were collected. The data were processed to obtain estimates of the MT impedance tensor [G. D. Egbert, *Geophys. J. Int.* **130**, 475 (1997)] and analyzed with tensor decomposition to determine if a 2D interpretation is valid [G. W. McNeice, A. G. Jones, *Geophysics* **66**, 158 (2001)].
12. Figures 2 and 3 show uniformly processed 2D conductivity models obtained from an inversion algorithm that generated the smoothest model consistent with the data [W. Rodi, R. L. Mackie, *Geophysics* **66**, 174 (2001)]. The inversion used the responses computed from electric currents flowing across geological strike (transverse magnetic, or TM, mode). TM responses have the advantage that they are usually less sensitive to 3D effects than the transverse electric (TE) mode responses, where electric currents flow parallel to strike [P. W. Wannamaker, G. W. Hohmann, S. Ward, *Geophysics* **49**, 1517 (1984)]. However, TM data are insensitive to narrow, near-vertical structures, and thus conductances derived from TM data alone are minimum estimates. Details of the inversion and figures showing the fit to the data are included in the supplementary material (*33*).
13. A. G. Jones, in *The Continental Lower Crust*, D. Fountain, R. J. Archulus, R. Kay, Eds. (Elsevier, Amsterdam, 1992), chap. 3.
14. Conductance is the product of conductivity and thickness and is well constrained by MT. However, MT does not readily distinguish separate combinations of conductivity and thickness. In parts of Tibet, the conductance of the midcrust is so high that the base of the conductive zone cannot be sensed and the upper conductance bound remains unknown. Thus, conductances in Figs. 2 and 3 are lower bounds.
15. M. L. Hauck, K. D. Nelson, L. D. Brown, W. Zhao, A. Ross, *Tectonics* **17**, 481 (1998).
16. C. Lemonnier *et al.*, *Geophys. Res. Lett.* **26**, 3261 (1999).
17. M. Hochstein, K. Regenauer-Lieb, *J. Volcanol. Geotherm. Res.* **83**, 75 (1998).
18. S. Turner *et al.*, *Nature* **364**, 50 (1993).
19. S. Willett, C. Beaumont, *Nature* **369**, 642 (1994).
20. B. Meyer *et al.*, *Geophys. J. Int.* **135**, 1 (1998).
21. B. R. Frost, W. S. Fyfe, K. Tazaki, T. Chan, *Nature* **340**, 134 (1989).
22. G. M. Partsch, F. R. Schilling, J. Arndt, *Tectonophysics* **317**, 189 (2000).
23. G. R. Olhoeft, *J. Geophys. Res.* **86**, 931 (1986).
24. J. J. Roberts, J. Tyburczy, *J. Geophys. Res.* **104**, 7055 (1999).
25. F. Schilling, G. Partzch, H. Brasse, G. Schwartz, *Phys. Earth. Planet. Inter.* **103**, 17 (1997).
26. R. D. Hyndman, P. M. Shearer, *Geophys. J. Int.* **98**, 343 (1989).
27. D. Alsdorf, K. D. Nelson, *Geology* **27**, 943 (1999).
28. J. Li, B. V. Miller, K. D. Nelson, S. D. Samson, *Eos* **79**, S344 (1998).
29. P. Henry, X. LePichon, B. Goffe, *Tectonophysics* **273**, 31 (1997).
30. M. Holness, *Contrib. Mineral. Petrol.* **131**, 68 (1998).
31. T. J. Owens, G. Zandt, *Nature* **387**, 37 (1997).
32. B. R. Hacker *et al.*, *Science* **287**, 2463 (2000).
33. Supplementary data are available on *Science* Online at www.sciencemag.org/cgi/content/full/292/5517/716/DC1.

34. INDEPTH MT fieldwork was made possible by support from the Ministry of Geology and Mineral Resources of the People's Republic of China, the NSF (Continental Dynamics Program), and the National Science Foundation of China.

5 December 2000; accepted 19 March 2001